Journal of Integrative Agriculture 2026, 25(7): 3006–3016

Available online at ScienceDirect

Journal of Integrative Agriculture



RESEARCH ARTICLE

Biochar amendment reduced microbial necromass carbon accumulation in a paddy soil profile

Ruiling Ma[1, 2], Suping Ji[1, 2], Shuo Jiang[1, 2], Dingyao Lei[1, 2], Ying Cai[1, 2], Xiulan Wu[1, 2], Zhiwei Liu[1, 2], Qi Yi[1, 2], Shaopan Xia[1, 2], Rongjun Bian[1, 2], Xuhui Zhang[1, 2], Jufeng Zheng[1, 2#]

[1] *Institute of Resource, Ecosystem and Environment of Agriculture, Nanjing Agricultural University, Nanjing 210095, China*
[2] *Jiangsu Collaborative Innovation Center for Solid Organic Waste Resource Utilization, Nanjing 210095, China*

Highlights

- Biochar reduced fungal necromass carbon in the topsoil while decreasing bacterial necromass carbon throughout the paddy soil profile.
- Biochar shifted the microbial community toward *K*-strategists to decrease microbial necromass carbon production.
- Biochar intensified microbial nitrogen limitation to enhance microbial necromass carbon decomposition.

Abstract

Microbial necromass carbon (MNC) serves a crucial function in the formation and stabilization of soil organic carbon (SOC). Although biochar amendment is recognized as a promising approach for enhancing SOC sequestration, its impact on MNC accumulation across the paddy soil profile remains uncertain. Through a 4-year field experiment, this study examined the effect of biochar amendment on MNC accumulation across three soil layers (0–15, 15–30, and 30–45 cm) in a paddy soil profile by combining vertical soil profiling, microbial community dynamics, and biomarker analysis. The results showed that biochar amendment reduced MNC by 10.5% (0–15 cm), 7.5% (15–30 cm), and 9.6% (30–45 cm), respectively, compared to the unamended control. In the topsoil (0–15 cm), the reduction in MNC under biochar amendment was attributed to decreases in both fungal and bacterial necromass carbon (C), whereas in the subsoil (15–45 cm), it primarily resulted from the decrease in bacterial necromass C. Biochar amendment reduced MNC content by decreasing microbial biomass and increasing nitrogen (N) acquisition enzyme activities, mainly due to a shift in the microbial community toward *K*-strategists and intensified microbial N limitation. This study provides novel insights into the microbially-mediated SOC dynamics in response to biochar amendment.

Keywords: biochar, microbial necromass carbon, microbial life-history strategy, paddy soil profile

1. Introduction

Soil organic carbon (SOC) is widely recognized as the primary contributor to crop production (Ma Y Q *et al.* 2023) and the maintenance of soil health (Weng *et al.* 2021). As the “engine” driving SOC transformation, soil microorganisms facilitate both SOC decomposition through extracellular enzyme secretion and SOC formation by converting organic substrates into microbial necromass through cycles of growth, reproduction, and death (Liang *et al.* 2017). Microbial necromass carbon (MNC), which stabilizes through chemical association with mineral surfaces (Buckeridge *et al.* 2020a) or physical occlusion within soil aggregates (Li *et al.* 2023), represents a relatively stable SOC fraction. In croplands, MNC constitutes 50.9 and 34.2% of SOC in the topsoil and subsoil (Takele *et al.* 2025), respectively, forming a major component of the soil carbon (C) pool (Liang *et al.* 2019; Huang *et al.* 2023; Yang *et al.* 2025). Therefore, understanding MNC dynamics is crucial for optimizing soil C management practices to mitigate climate change and advance C neutrality goals.

Biochar amendment has emerged as a promising approach for enhancing SOC stability (Wang *et al.* 2016;

Received 12 May 2025; Received in revised form 27 August 2025; Accepted 15 September 2025; Available online 1 October 2025
Ruiling Ma, E-mail: mrlashore@163.com; #Correspondence Jufeng Zheng, Tel: +86-25-84399852, E-mail: zhengjufeng@njau.edu.cn

© 2026 CAAS. Publishing services by Elsevier B.V. on behalf of KeAi Communications Co. Ltd. This is an open access article under the CC BY-NC-ND license (http://creativecommons.org/licenses/by-nc-nd/4.0/). Peer review under responsibility of Editorial Board of *Journal of Integrative Agriculture*.
doi: 10.1016/j.jia.2025.10.001

Wang J X *et al.* 2024), increasing SOC sequestration (Sohi 2012), and mitigating climate change (Lehmann *et al.* 2021). Through its effects on soil nutrient availability (Yao *et al.* 2017) and soil structure modification (Feng *et al.* 2022; Chen *et al.* 2025), biochar amendment influences microbial community composition, interactions and activities (Lei *et al.* 2023), thereby affecting the trade-off between production and decomposition of MNC (Chen *et al.* 2023b). For instance, nutrient enrichment from biochar could improve microbial biomass and C use efficiency (Liu *et al.* 2020). Additionally, by modulating interactions among key taxa within microbial co-occurrence networks (Zhang *et al.* 2024; Wang *et al.* 2025), biochar could select for r-strategists that flourish in nutrient-rich environments and exhibit high biomass turnover (Kerner *et al.* 2023), potentially increasing MNC production (Zhang *et al.* 2024). However, nutrients associated with biochar particles undergo rapid mineralization and depletion (Nan *et al.* 2023). The remaining C fractions, characterized by high aromaticity and low bioavailability, are resistant to microbial utilization and may favor *K*-strategists. These microorganisms specialize in degrading complex substrates while maintaining low microbial biomass, potentially reducing MNC production under biochar amendment (Chen *et al.* 2023a). Indeed, previous research demonstrated that biochar reduced MNC by shifting microbial community towards *K*-strategists in a paddy topsoil (Zhu *et al.* 2025). Moreover, excessive C inputs from biochar may disrupt soil stoichiometry and alter microbial nutrient acquisition strategies (Gao *et al.* 2019). A meta-analysis indicated that high C/N ratio of biochar intensified microbial nitrogen (N) limitation and increased the ratio of N-acquiring to C- and phosphorus (P)-acquiring enzyme activities (Chen *et al.* 2022). Given the elemental and chemical similarity between microbial necromass and living microbial biomass (Buckeridge *et al.* 2022), biochar-induced N limitation may accelerate MNC decomposition to satisfy microbial N requirements (Yang *et al.* 2024). However, effect of biochar amendment on the trade-off between MNC production and decomposition remains inadequately understood and requires further investigation.

Rice paddies, encompassing 167 million ha worldwide (Liu Y L *et al.* 2019), demonstrate higher SOC sequestration efficiency than adjacent upland soils (Chen *et al.* 2021) and store approximately 18 Pg C in the 0–100 cm soil profile (Liu Y L *et al.* 2021). While biochar application has been demonstrated to increase rice yield (Xia *et al.* 2023), reduce greenhouse gas emissions (Jiang *et al.* 2023), and enhance SOC sequestration (Xia *et al.* 2023) in paddy soils, research has primarily focused on topsoil (Liu Z W *et al.* 2019; Zhu *et al.* 2025), where abundant rhizodeposits and high fertilizer inputs favor r-strategists that exhibit rapid microbial biomass turnover (Li Z *et al.* 2024; Cao *et al.* 2025). In comparison, subsoil receives limited plant-derived C and nutrient inputs but provides stronger mineral sorption and physical protection of organic matter (Qin *et al.* 2019). These conditions favor *K*-strategists, slow microbial C turnover, and promote the accumulation of more chemically recalcitrant C (Huang *et al.* 2023), resulting in depth-dependent responses of MNC to biochar addition. For instance, under frequent dry-wet alternation, biochar may disintegrate and migrate to depths of 10–140 cm in the paddy soil profile (Major *et al.* 2010; Koele *et al.* 2017; Jia *et al.* 2024), potentially increasing dissolved organic carbon (DOC) aromaticity and shifting microbial communities towards *K*-strategists while decreasing microbial biomass (Ma R L *et al.* 2023; Wang Y *et al.* 2024). Furthermore, by limiting downward nutrient flux from topsoil (Shi *et al.* 2020) and enhancing nutrient uptake by rice roots in deeper layers (Kong *et al.* 2024), biochar amendment may intensify nutrient deficiencies and accelerate microbial turnover of MNC in paddy subsoil. Consequently, biochar application may significantly alter microbial community and nutrient acquisition strategies in the subsoil, ultimately affecting MNC accumulation. While biochar's effect on MNC accumulation in topsoil has been increasingly studied (Chen *et al.* 2023a; Zhang *et al.* 2024), its impact across the paddy soil profile remains unclear.

To address this knowledge gap, we conducted a 4-year field experiment to investigate the effects of biochar amendment on MNC accumulation across three soil layers (0–15, 15–30, and 30–45 cm) in a paddy soil profile. Soil samples were collected from control and biochar-amended plots, and MNC accumulation was evaluated through amino sugar analysis. Microbial abundance and community structure were assessed using phospholipid fatty acid (PLFA) analysis and DNA sequencing. Our previous research indicated that biochar reduced MNC accumulation by shifting microbial communities towards *K*-strategists two years after application (Zhu *et al.* 2025). Additionally, biochar aging can increase surface area and introduce more oxygen-containing functional groups, thereby enhancing sorption capacity and reducing downward N flux (Shi *et al.* 2020). Therefore, we hypothesize that four years after a single application (1) biochar amendment would decrease MNC accumulation by exacerbating N limitation and suppressing microbial biomass in the paddy soil profile; and (2) bacterial necromass carbon (BNC) and fungal necromass carbon (FNC) would respond differently to biochar addition due to distinct nutrient-acquisition strategies of bacterial versus fungal communities.

2. Materials and methods

2.1. Experiment description and soil sampling

The experiment was conducted in a rice paddy located in Yixing County, Jiangsu Province, China (31°24′N, 119°41′E) beginning in May 2016. The region experiences a subtropical monsoon climate with a mean annual temperature of 16°C and mean annual precipitation of 1,230.6 mm. The experimental paddy field soil was classified as a Hydroagric Stagnic Anthrosol (Gong 1999). The experiment included two treatments with three replicates: biochar amended at 15 t ha^{-1} (BC) and biochar unamended control (CK). Each experimental plot shared 20 m^2 (4 m×5 m). The biochar, produced from maize straw pyrolysis at 450°C, was uniformly incorporated into the plow layer (0–15 cm) through mechanical rotary tillage before rice cultivation in 2016. Biochar application occurred once in 2016, with no subsequent applications. The planting system was rice–

wheat rotation. Annual fertilizer applications during the rice season consisted of 200 kg N ha^{-1} as urea, 50 kg ha^{-1} P_2O_5 as $Ca(H_2PO_4)_2$, and 50 kg ha^{-1} K_2O as KCl, while the wheat season received 100 kg N ha^{-1}, 38 kg ha^{-1} P_2O_5, and 33 kg ha^{-1} K_2O. The basic properties of the topsoil (0–15 cm) and biochar are presented in Appendix A.

Four years after biochar amendment, rice roots were randomly sampled from 15 hills in each treatment following rice harvest in October 2020. The root samples were rinsed with ultrapure water, dried at 80°C to constant mass, and weighed. Five soil samples were collected from each plot using a 5-cm diameter steel corer to a depth of 45 cm. The samples were separated into three depth categories: 0–15, 15–30, and 30–45 cm. Samples from identical depths within each plot were thoroughly mixed *in-situ* to create composite samples. In total, 18 soil samples were collected (2 treatments×3 replicates×3 depths). All soil samples were immediately transported to the laboratory. After removing visible roots and rocks, the soil samples were passed through a 2 mm sieve and divided into three subsamples: one for microbial community composition analysis (stored at −80°C); one for soil extracellular enzymes, DOC, NH_4^+, and NO_3^- assessment (stored at 4°C); and one for soil chemical properties, microbial biomass (indicated by PLFA) and amino sugar measurement (freeze-dried and stored at room temperature).

2.2. Analysis of soil chemical properties

Soil chemical properties were analyzed according to Bao (2000). Soil pH was measured using a standard pH meter in a 1:2.5 soil:water suspension. SOC and total N (TN) were determined using an elemental analyzer (Thermo Fisher Scientific, FLASH 2000 CHNS/O, America). Soil available phosphorus (AP) was extracted using 0.5 mol L^{-1} $NaHCO_3$ and analyzed using the molybdenum-antimony antispectrophotometric method. Soil available potassium (AK) was extracted using 0.5 mol L^{-1} CH_3COONH_4 and measured by flame spectrophotometer. Soil DOC was extracted with deionized water and analyzed using a total organic C analyzer (Multi N/C 3000; Analytik Jena, Germany). $SUVA_{254}$ of DOC was measured using a UV-A360 spectrophotometer (AOYI, Shanghai, China) (Li and Hur 2017). Soil available N (AN) (NO_3^- and NH_4^+) was extracted by 2 mol L^{-1} KCl and measured using a flow analyzer (AA3, SEAL). The DOC to AN ratio was calculated to represent the relative availability of C to N.

2.3. Analysis of amino sugars and microbial necromass C

Soil amino sugars, including glucosamine (GluN), muramic acid (MurA), and galactosamine (GalN), were measured following the methodology described by Zhang and Amelung (1996). Specifically, freeze-dried soil sample (containing approximately 0.4 mg N) underwent hydrolysis at 105°C for 8 h with 6 mol L^{-1} HCl. After adding 100 μg myo-inositol, the solution was filtered. Amino sugars were collected with methanol and evaporated using N_2 gas after lyophilization. The residue was dissolved in derivatization reagent and heated at 75–80°C for 35 min. The derivatives underwent acetylation and thorough washing with deionized water three times before drying using N_2 gas at 45°C. Finally, the amino sugar derivatives were re-dissolved in ethyl acetate-hexane and analyzed using the Agilent 7890B GCMS (Agilent Technologies, Santa Clara, CA, USA).

FNC and BNC were calculated according to previous studies (Appuhn and Joergensen 2006; Joergensen 2018) (Appendix B):

$$\text{FNC (mg kg}^{-1}) = \left(\frac{\text{GluN}}{179.17} - 2\times\frac{\text{MurA}}{251.23}\right)\times 179.17\times 9\times 1{,}000 \quad (1)$$

$$\text{BNC (mg kg}^{-1}) = \text{MurA}\times 45\times 1{,}000 \quad (2)$$

The values 9 and 45 represent the conversion factors for GluN to FNC and MurA to BNC, respectively. The values 179.17 and 251.23 represent the molecular weights of GluN and MurA, respectively. Total MNC content was calculated as the sum of FNC and BNC.

2.4. Analysis of soil enzymatic activities

The activities of phenol oxidase (PO), β-1,4-glucosidase (BG), β-1,4-cellobiohydrolase (CEB), β-1,4-N-acetylglucosaminidase (NAG), and acid phosphatase (ACP), which are involved in C, N, and P transformation, were measured using the methods of German *et al.* (2011) and Bach *et al.* (2013) with minor modifications. Specifically, 2.4 g of fresh bulk soil (sieved to 2 mm) was mixed with 300 mL of buffer solution to form a homogeneous slurry. For hydrolases, 200 μL of the slurry were mixed with the 50 μL of 200 μmol L^{-1} substrate in a black 96-well polystyrene plate and incubated in the dark at 25°C for 3 h. For PO, 1,000 μL of soil slurry was combined with 50 μL of 25 mmol L^{-1} L-DOPA in a 2 mL centrifuge tube and incubated in the dark at 30°C for 6 h. Fluorescence for BG, CEB, ACP and NAG was measured with excitation at 365 nm and emission at 450 nm, while absorbance for PO was measured at 450 nm using a microplate reader (MDS Analytical Technologies, Molecular Devices, USA). The enzyme activities were expressed as nmol g^{-1} dry soil h^{-1}.

2.5. Analysis of soil microbial biomass

Soil microbial biomass was assessed through phospholipid fatty acids (PLFAs) and quantified using the method developed by Bossio and Scow (1998). Specifically, freeze-dried soil sample (2 g) was extracted with a chloroform/methanol/citric buffer (0.15 mol L^{-1}, pH 4.0) mixture. The extracted lipids were separated into neutral lipids, glycolipids, and phospholipids using a silica-bonded phase column. After adding methyl nonadecanoate (19:0) as an internal standard, the solvent was evaporated under nitrogen gas. The fatty acid methyl esters (FAMEs) were obtained by adding a methanol solution to the residue. The FAMEs were analyzed using the Agilent 7890B GCMS (Agilent Technologies, Santa Clara, CA, USA). The specific PLFA biomarkers used in this study are shown in Appendix C.

2.6. Analysis of soil microbial community composition and co-occurrence network

Soil microbial community composition was characterized

through bacterial 16S rRNA and fungal internal transcribed spacer (ITS) gene sequencing, as described in our previous study (Ma R L *et al.* 2023). Soil genomic DNA was extracted using the PowerSoil® DNA Isolation Kit (Mo Bio Laboratories Inc., CA). The bacterial 16S rRNA and fungal ITS genes were amplified using primer sets 338F/806R and ITS3-KYO2/ITS4, respectively. Following purification, 16S rRNA and ITS gene sequencing was conducted using the Illumina Miseq PE300 sequencing platform (Illumina, Inc., San Diego, CA, USA). Raw sequence reads were filtered, trimmed, and merged using VSEARCH (version 2.7.1). Operational taxonomic units (OTUs) were generated with a 97% sequence identity similarity threshold using UPARSE algorithm. The OTUs were then classified using SILVA (version 138) and UNITE (version 8.2) databases for 16S rRNA and ITS regions, respectively. The raw sequencing data have been deposited in the NCBI database (SRA) with accession number of PRJNA1229827. The bacterial and fungal communities were classified into r-strategists and *K*-strategists at the phylum level (Appendix D) based on previous studies (Li *et al.* 2021; Shao *et al.* 2021; Cai *et al.* 2023; Hu *et al.* 2023). The r/*K* ratio was calculated as the sum of r-strategists divided by the sum of *K*-strategists. Additionally, 16S rRNA (*rrn*) operon copy number was used as a trait-based, taxonomy-independent proxy for microbial r/*K* strategies (Li *et al.* 2021; Hu *et al.* 2023). OTU-level *rrn* operon copy numbers were obtained from the *rrn*DB database, and community-weighted mean *rrn* operon copy numbers were calculated for each sample by multiplying each OTU's *rrn* operon copy number by its relative abundance and summing across OTUs.

Co-occurrence network analysis at the OTU level was conducted using the R package "igraph" (Ju *et al.* 2014). The statistical threshold was established as Pearson's correlation coefficient (r)>0.8 and P<0.01 (Barberán *et al.* 2012; Fan *et al.* 2019). Network visualization and topology parameter calculations were performed using Gephi (version 0.9.7). Each network node represented an OTU, with edges indicating significant correlations between nodes. Module abundance was calculated by averaging the relative abundance of species within each module (Fan *et al.* 2019). The relative abundances of r-strategists and *K*-strategists in each module were calculated by summing the relative abundances of species classified as r- or *K*-strategists at the phylum level (Han *et al.* 2023).

2.7. Statistical analyses

Prior to data analysis, data were evaluated for homogeneity of variance and normality using Levene's test and Shapiro-Wilk test, respectively. Significant differences in measured parameters across soil depths were evaluated using one-way ANOVA, followed by the Tukey test. Independent sample *t*-tests were conducted to assess differences in measured parameters between CK and BC within each soil depth. Permutational multivariate analysis of variance (PerMANOVA) was performed using "vegan" to examine differences in microbial community structure among treatments. STAMP (version 2.1.3) was employed to determine statistical differences at phylum levels (Parks *et al.* 2014). Benjamini-Hochberg FDR correction was applied to adjust *P*-values from *t*-tests, PerMANOVA, and linear regressions. The significance of microbial co-occurrence network modules' effects on MNC was assessed through random forest analysis using the "randomForest" and "rfPermute" R packages. The mean square errors (%IncMSE) of network modules were compared to evaluate each module's importance in driving MNC variations. All data analyses were conducted and visualized using R 4.2.1 software (R Core Team 2022).

3. Results

3.1. Soil chemical properties

The influence of biochar addition on soil chemical properties varied with depth (Table 1). Biochar application increased the concentrations of SOC and DOC in both 0–15 and 15–30 cm soil layers. The $SUVA_{254}$ of DOC was increased by 11.8, 12.5, and 22.7% in the 0–15, 15–30, and 30–45 cm soil layers, respectively, after biochar amendment. However, biochar decreased AN content by 11.6 and 20.1% in the 15–30 and 30–45 cm soil layers, respectively. Furthermore, biochar amendment raised soil pH from 5.68 to 6.29 in the 0–15 cm soil layer. Soil C/N and DOC/AN ratios was improved by biochar amendment in the 0–15 and 15–30 cm soil layers.

3.2. Soil microbial necromass carbon

Biochar amendment exhibited varying effects on FNC and BNC throughout the soil profile (Fig. 1-B and C). In the 0–15 cm soil layer, biochar application significantly decreased BNC and FNC by 10.9 and 8.8%, respectively, compared to the control. However, in the 15–30 and 30–45 cm soil layers, FNC remained unchanged, while BNC was decreased by

Table 1 Soil chemical properties of the control and biochar-amended treatments in different soil layers[1)]

Depth (cm)	Treatment[2)]	pH (H_2O)	SOC (g kg^{-1})	TN (g kg^{-1})	C/N	DOC (mg kg^{-1})	AN (mg kg^{-1})	DOC/AN	AP (mg kg^{-1})	AK (mg kg^{-1})	$SUVA_{254}$ (L mg^{-1} m^{-1})
0–15	CK	5.7 Bc	24.2 Ba	2.0 Aa	12.0 Ba	132 Ba	45 Aa	2.9 Bb	24.7 Aa	96.3 Aa	2.5 Ba
	BC	6.3 Ac	28.9 Aa	2.0 Aa	14.4 Aa	169 Aa	44 Aa	3.9 Ab	26.3 Aa	94.2 Aa	2.7 Aa
15–30	CK	6.3 Ab	12.8 Bb	0.9 Ab	14.2 Ba	116 Bb	19 Ab	6.1 Ba	15.7 Ab	63.1 Ab	2.1 Bb
	BC	6.4 Ab	14.7 Ab	1.0 Ab	15.4 Aa	131 Ab	17 Bb	7.8 Aa	14.8 Ab	62.4 Ab	2.4 Ab
30–45	CK	6.7 Aa	7.6 Ac	0.6 Ac	13.4 Aa	91 Ac	20 Ab	4.5 Aa	6.4 Ac	52.3 Ac	1.8 Bc
	BC	6.8 Aa	7.4 Ac	0.5 Ac	14.6 Aa	102 Ac	16 Bb	6.4 Aa	7.8 Ac	51.5 Ac	2.2 Ac

[1)] SOC, soil organic carbon; TN, total nitrogen; C/N, the ratio of soil organic carbon to total nitrogen; DOC, dissolved organic carbon; AN, available nitrogen; DOC/AN, the ratio of dissolved organic carbon to available nitrogen; AP, available phosphorus; AK, available potassium.
[2)] CK and BC represent the control and biochar-amended treatment, respectively.
Values are the means (n=3). Different capital letters denote significant difference between CK and BC in the same soil layer (P<0.05). Different small letters denote significant difference among different soil layers (P<0.05).

biochar amendment by 19.5 and 32.8%, respectively. As a result, biochar decreased MNC by 10.5, 7.5, and 9.6% in the 0–15, 15–30, and 30–45 cm soil layers, respectively (Fig. 1-A). Additionally, the FNC/BNC ratio was increased under biochar amendment in the 15–30 and 30–45 cm soil layers (Fig. 1-D).

3.3. Soil microbial biomass and enzymatic activities

Bacterial and fungal PLFAs showed distinct responses to biochar amendment across the soil profile (Fig. 1-F and G). In the 0–15 cm soil layer, biochar amendment decreased fungal and bacterial PLFAs by 25.3 and 9.1%. In the 15–30 and 30–45 cm soil layers, fungal PLFAs remained unchanged, while bacterial PLFAs was decreased by 8.5 and 8.9%, respectively. Consequently, biochar amendment reduced total microbial PLFAs by 11.3, 9.4, and 9.4% in the three soil layers (Fig. 1-E). Furthermore, F/B was decreased by biochar amendment in the 0–15 cm soil layer (Fig. 1-H).

Biochar amendment decreased C acquisition enzyme activities, enhanced N acquisition enzyme activities, but showed no impact on P acquisition enzyme activity across depths (Fig. 1-I–M). Specifically, biochar decreased the BG and CEB activity by 13.6–40.4 and 19.1–24.2%, respectively, in the 0–15 and 15–30 cm soil layers compared to the control (Fig. 1-I and J). Moreover, biochar addition reduced PO activity by 8.2 and 14.7% in the 15–30 and 30–45 cm soil layer, respectively (Fig. 1-K). In contrast, biochar amendment improved NAG activity by 82.9–152.9% across the three soil layers (Fig. 1-L).

3.4. Soil microbial community structure and co-occurrence patterns

NMDS based on Bray-Curtis distance and PerMANOVA demonstrated that both soil depth and biochar amendment significantly modified soil bacterial and fungal community structure (Appendix E). In the 0–15 cm soil layer, biochar amendment increased the relative abundances of 4 bacterial phyla (Acidobacteria, Chloroflexi, Nitrospirae, Rokubacteria) and 2 fungal phyla (Basidiomycota, Glomeromycota) while decreasing the relative abundances of bacterial phylum Gemmatimonadetes and fungal phylum Ascomycota (Fig. 2-A and B). In the 15–30 cm soil layer, biochar addition

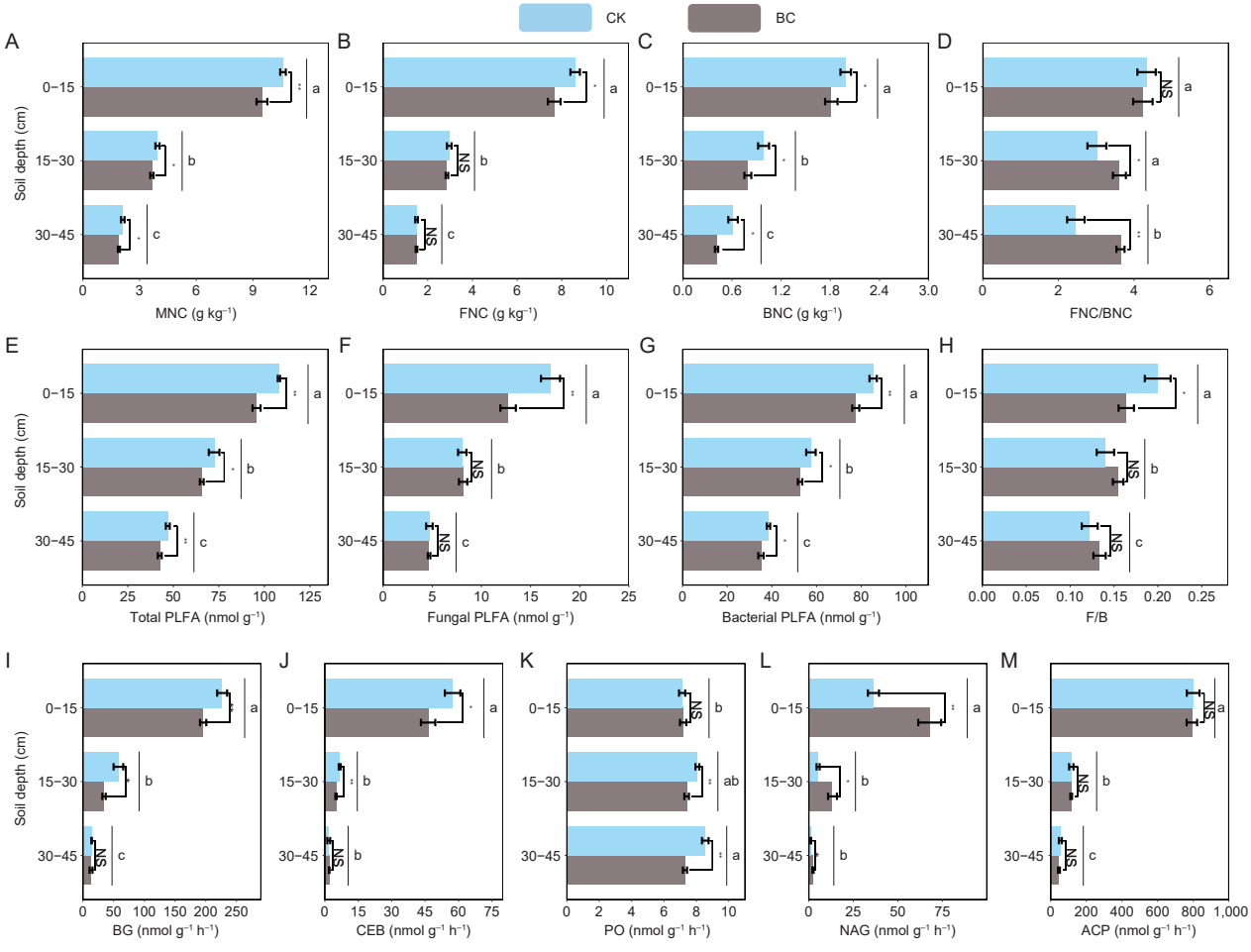


Fig. 1 Microbial necromass carbon (MNC), biomass, and extracellular enzyme activities under the control (CK) and biochar-amended (BC) treatment across soil layers. FNC, fungal necromass C; BNC, bacterial necromass C; FNC/BNC, the ratio of fungal necromass C to bacterial necromass C; F/B, the ratio of fungal PLFA to bacterial PLFA; BG, β-1,4-glucosidase; CEB, β-1,4-cellobiohydrolase; PO, phenol oxidase; NAG, β-1,4-N-acetylglucosaminidase; ACP, acid phosphatase. Different small letters denote significant difference among different soil layers (P<0.05). * and ** indicate significant difference between CK and BC in the same soil layer at P<0.05, P<0.01, respectively. Error bars represent the standard deviation of the means (n=3).

improved the relative abundances of 3 bacterial phyla (Firmicutes, Rokubacteria, Nitrospirae) but reduced the relative abundances of bacterial phylum Gemmatimonadetes and fungal phylum Ascomycota (Fig. 2-C and D). In the 30–45 cm soil layer, biochar addition increased the relative abundances of 2 bacterial phyla (Acidobacteria, Nitrospirae) and fungal phylum Basidiomycota but reduced the relative abundance of bacterial phylum Actinobacteria (Fig. 2-E and F). Except for the bacterial community at 15–30 cm soil layer, biochar amendment enhanced the *K*/r of fungal and bacterial communities across the soil profile (Appendix F).

Co-occurrence networks were constructed to illustrate the distinct co-occurrence patterns of soil microbial communities following biochar amendment. The bacterial network comprised 1,395 nodes and 55,155 links (Fig. 3-A), while the fungal network contained 155 nodes and 352 links (Fig. 3-B). Both networks were clustered into five coherent modules. Random forest modeling revealed that MNC was significantly influenced by bacterial module 1, bacterial module 3, bacterial module 5 and fungal module 3 (R^2=0.81; P=0.001; Fig. 3-C). By calculating relative abundances of r-strategists and *K*-strategists in each module, we found that bacterial modules 1 and 5 were dominated by *K*-strategists while bacterial module 3 was dominated by r-strategists (Fig. 3-D). Furthermore, although fungal module 3 was dominated by r-strategists, it demonstrated a higher proportion of *K*-strategists compared to other fungal modules (Appendix G). Consequently, bacterial module 3 was classified as r-strategist-dominated, while bacterial modules 1 and 5, along with fungal module 3, were designated as *K*-strategist-dominated modules. Linear regression analyses demonstrated that MNC positively correlated with the relative abundance of the r-strategist bacterial module 3, but negatively correlated with the relative abundances of the *K*-strategist modules (bacterial modules 1 and 5, and fungal module 3) (Fig. 3-E–H).

4. Discussion

The net accumulation of MNC depends on the balance among microbial biomass production, microbial mortality, and the decomposition of microbial residues (Joergensen 2018; Liang *et al.* 2019). In contrast to previous studies reporting increased MNC accumulation under biochar amendment (Chen *et al.* 2023a; Cheng *et al.* 2024; Yuan *et al.* 2025), this study found that biochar reduced MNC content throughout the paddy soil profile (Fig. 1-A), supporting our first hypothesis. The reduction in MNC under biochar amendment appears to be associated with two mechanisms (Fig. 4): (i) biochar shifted the microbial community towards *K*-strategist, suppressing microbial biomass and decreasing MNC production; and (ii) biochar intensified microbial N limitation and stimulated NAG activities, thereby enhancing MNC decomposition.

4.1. Biochar amendment decreased microbial necromass carbon production by shifting microbial life-history strategy

In contrast to previous studies indicating that biochar stimulates microbial biomass and increases MNC accumulation (Li M R *et al.* 2024; Yuan *et al.* 2025), this study

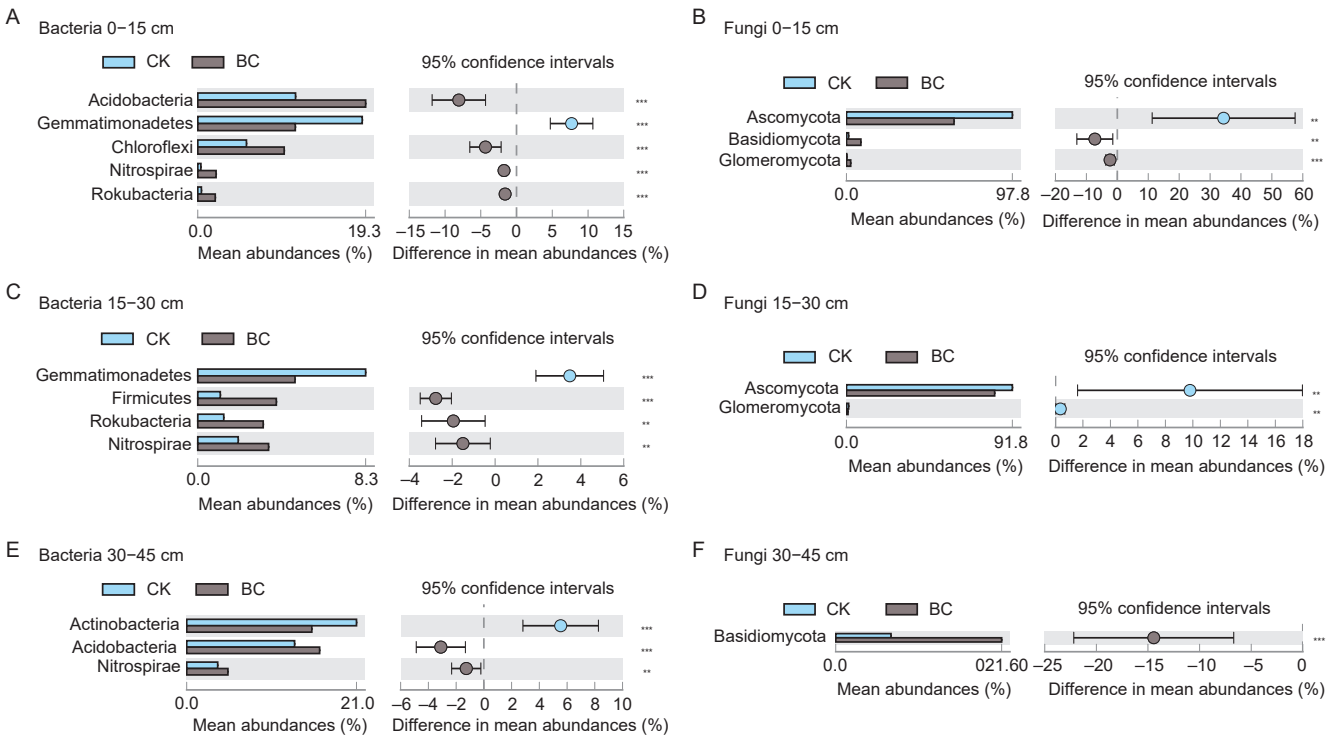


Fig. 2 The relative abundances of microbial phyla with significant changes under the control (CK) and biochar-amended (BC) treatment across soil layers. *, **, and *** indicate significant difference between CK and BC in the same soil layers at P<0.05, P<0.01, and P<0.001, respectively.

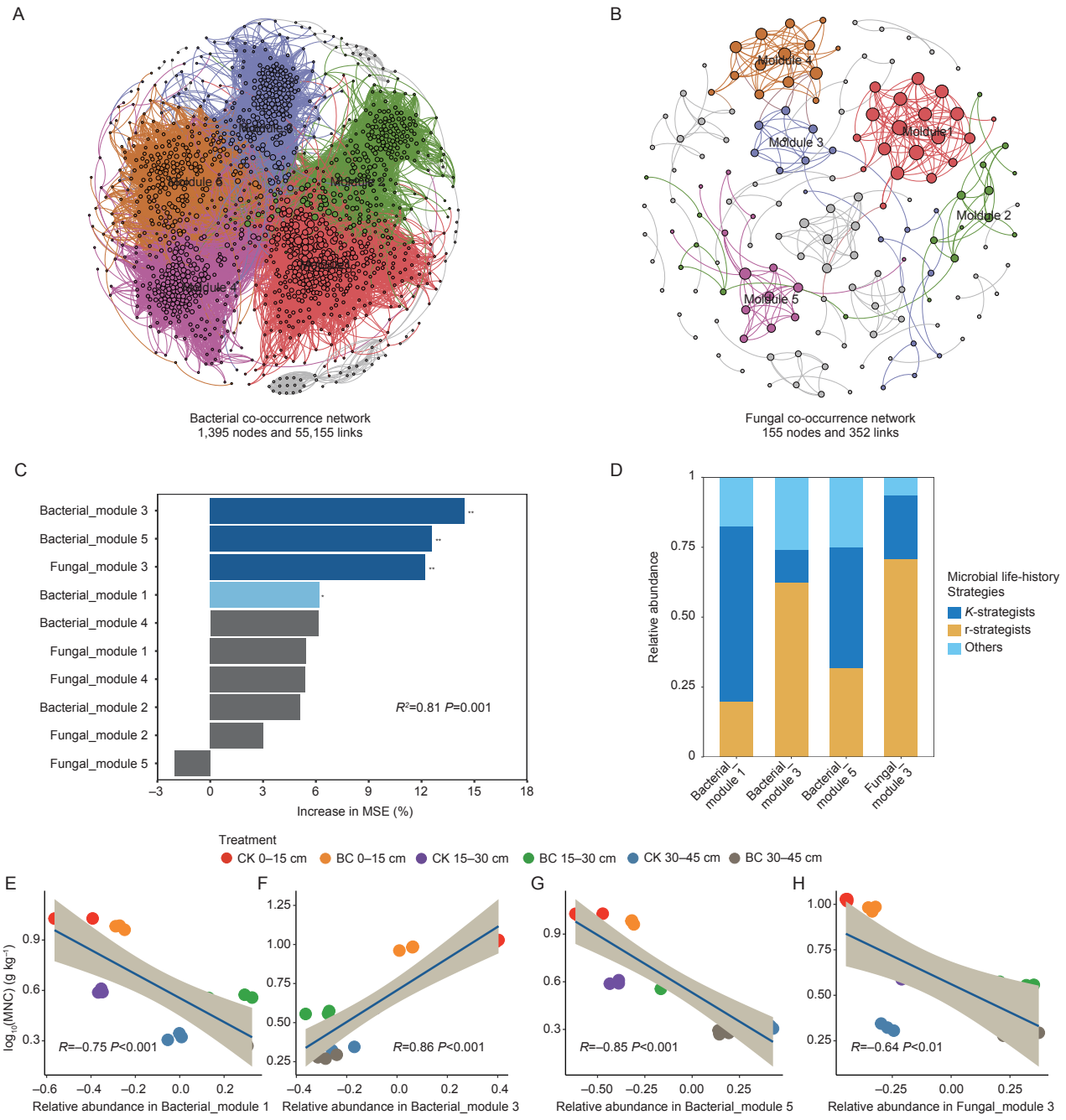


Fig. 3 Key microbial modules regulating microbial necromass carbon (MNC) accumulation. A, bacterial co-occurrence network. B, fungal Co-occurrence network. C, key modules identified by random forest model. D, relative abundances of different life-history strategists in key modules. E–H, relationships between key modules and MNC. CK, control; BC, biochar-amended treatment.

observed a significant decline in microbial biomass across all three soil layers four years after a single biochar application (Fig. 1-E). This pattern may be attributed to the biochar-induced shift in microbial life-history strategies. Generally, r-strategists thrive in nutrient-rich environments and exhibit rapid biomass turnover, while *K*-strategists predominate under nutrient-limited or imbalanced conditions by reducing biomass turnover and utilizing recalcitrant substrates (Fierer *et al.* 2007; Malik *et al.* 2020). Unlike previous studies employing annual biochar applications (Zhang *et al.* 2024; Yuan *et al.* 2025), this experiment utilized a single biochar application. Under frequent wetting and drying cycles in paddy soils, the readily available nutrients from the one-time biochar application may have been consumed by rice and microbes (Nan *et al.* 2023). Additionally, biochar amendment increased $SUVA_{254}$ values of DOC (Table 1), indicating enhanced aromaticity and reduced bioavailability (Li and Hur 2017). This observation aligns with previous research demonstrating that SOC and DOC exhibit higher aromaticity and greater resistance to microbial utilization 14 years after biochar application (Chen *et al.* 2023a). Consequently, biochar fractions in the soil profile primarily consisted of

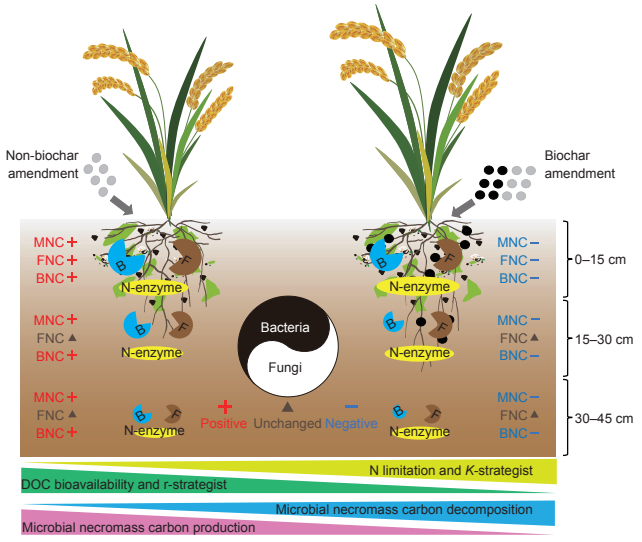


Fig. 4 Conceptual diagram of the accumulation of microbial necromass carbon (MNC) under the control and biochar-amended treatment across soil layers. FNC, fungal necromass carbon; BNC, bacterial necromass carbon; B, bacterial biomass; F, fungal biomass; N-enzyme, N-acquisition enzyme (β-1,4-N-acetylglucosaminidase).

recalcitrant C, potentially favoring *K*-strategist proliferation while inhibiting r-strategists (Li *et al.* 2021).

This study revealed that biochar application increased the relative abundances of *K*-strategists (e.g., Nitrospirae and Basidiomycota) while decreasing those of r-strategists (e.g., Gemmatimonadetes and Ascomycota) across soil layers (Fig. 2), resulting in higher microbial *K*/r ratios and lower *rrn* operon copy numbers (Appendix F). Co-occurrence network analysis confirmed this pattern, demonstrating that biochar suppressed r-strategy modules while enhancing *K*-strategy core modules (Fig. 3; Appendix H), indicating a community shift toward *K*-strategists in the soil profile. This low-yield, slow-turnover, and oligotrophic microbial community induced by biochar amendment decreased microbial biomass inputs to the necromass pool (Fig. 1-E) (Shao *et al.* 2021; Cai *et al.* 2023), as microbial biomass serves as the immediate precursor of necromass (Buckeridge *et al.* 2020b). Notably, fungal and bacterial biomass showed distinct responses to biochar amendment. The results indicated that biochar amendment reduced bacterial biomass across three soil layers (Fig. 1-G), while fungal biomass was decreased only in the topsoil (Fig. 1-F). The topsoil response likely reflects elevated pH under biochar amendment (Table 1), which typically inhibits fungal growth and metabolism while enhancing fungal chitin decomposition (Hu *et al.* 2020; Wang C *et al.* 2021). In the subsoil, however, the recalcitrant biochar-derived C may sustain fungal growth while limiting bacterial biomass, as fungi generally possess a competitive advantage in utilizing recalcitrant C substrates compared to bacteria (Lehmann *et al.* 2011; Lei *et al.* 2023). These findings indicate that the decline in MNC production in topsoil resulted from reductions in both fungal and bacterial biomass, whereas the subsoil decline was primarily attributed to decreased bacterial biomass under biochar amendment.

4.2. Biochar amendment accelerated microbial necromass carbon decomposition by aggravating microbial N limitation

N availability plays a crucial role in the recycling and destabilization of MNC (Hu *et al.* 2018; Buckeridge *et al.* 2020). According to the theories of stoichiometric homeostasis and microbial N mining, microorganisms mineralize SOM to meet their N requirements under N-limited conditions (Chen *et al.* 2014). Microbial necromass, as an N-abundant substrate (Heuck *et al.* 2015), is susceptible to microbial N mining (Hu *et al.* 2018; Cui *et al.* 2020). The present study demonstrated that biochar amendment indirectly intensified N limitation by increasing the DOC content and the DOC/AN ratio in the topsoil (Table 1). The increased DOC content under biochar amendment may be attributed to higher rice root biomass (Appendix I) and associated rhizodeposits (Liu Z W *et al.* 2021). In the subsoil (15–45 cm soil layers), biochar amendment reduced N availability by decreasing the AN content (Table 1), aligning with previous research showing reduced downward leaching of ^{15}N into deeper soil layers in a pot experiment (Shi *et al.* 2020). This reduction in AN may result from two factors. First, biochar can reduce N leaching from topsoil to subsoil through strong adsorption capacity, facilitated by abundant oxygen-containing functional groups (Gai *et al.* 2014), and its high porosity and large specific surface area that enhance water-holding capacity (Novak *et al.* 2012). Second, increased root biomass under biochar amendment (Appendix I) may promote deeper root penetration and intensify plant–microbe competition for AN in the subsoil (Liu *et al.* 2018; Hill and Jones 2019). However, sampling at rice harvest coincided with seasonally low mineral-N pools (Zhu *et al.* 2019). Following field drainage and a complete growing season of plant uptake, this timing may have accentuated the low AN level in the subsoil. Consequently, under biochar amendment, the combined effects of elevated root deposition and labile C supply in the topsoil, along with reduced AN in the subsoil, likely exacerbate microbial N limitation, thereby stimulating higher secretion of N-acquiring enzymes to mine N from soil organic matter — particularly from N-rich microbial necromass (Buckeridge *et al.* 2020b).

In alignment with these findings, our results demonstrated that biochar did not modify P acquisition activity but decreased C hydrolase activities (e.g., BG and CEB) and enhanced NAG in the soil profile (Fig. 1-I–M), suggesting relative microbial N limitation (Sinsabaugh *et al.* 2013). Furthermore, the relative abundance of Nitrospirae, an oligotrophic phylum critical for N transformation processes through nitrite oxidation (Dunbar *et al.* 2014; Daims and Wagner 2018), increased under biochar amendment (Fig. 2-A, C, and E), potentially mitigating N limitation and sustaining microbial functioning. Consequently, the intensified microbial N limitation and increased N acquisition activity could scavenge N from microbial residue and potentially accelerate MNC decomposition (Sinsabaugh *et al.* 2008; Buckeridge *et al.* 2020b). Moreover, biochar amendment reduced FNC primarily in the topsoil while decreasing BNC across all three soil layers (Fig. 1-B and C). This distinction can be attributed

to the molecular recalcitrance of fungal cell wall components, including chitin and melanin, which confer a longer turnover time compared to bacterial cell wall components such as peptidoglycans (Schweigert *et al.* 2015; Wang B G *et al.* 2021). The lower surface-area-to-volume ratios of fungal residues could facilitate their adsorption onto mineral surfaces, thereby enhancing fungal necromass preservation in mineral-rich subsoils (Schweigert *et al.* 2015; He *et al.* 2022). Conversely, bacterial necromass, characterized by lower molecular mass and C/N ratios, exhibits greater susceptibility to high NAG activity (Hu *et al.* 2020; Wang *et al.* 2022). Thus, FNC demonstrates greater resistance than BNC to elevated decomposition induced by biochar amendment, resulting in stable FNC accumulation in the subsoil. These results reveal distinct responses of BNC and FNC to biochar-induced microbial N limitation and subsequent enzymatic activity changes.

5. Conclusion

This study demonstrates that biochar amendment reduced MNC accumulation by modifying microbial life-history strategies and intensifying N limitation across the three paddy soil layers (0–15, 15–30, and 30–45 cm). Biochar amendment decreased DOC bioavailability and shifted the microbial community toward *K*-strategists, thereby reducing microbial biomass and potentially decreasing MNC production. Additionally, biochar intensified microbial N limitation and stimulated NAG activities, potentially accelerating MNC decomposition. As a result, biochar amendment reduced FNC mainly in the topsoil while decreasing BNC throughout all soil layers. These findings highlight the significance of microbial life-history strategy and N availability in regulating MNC dynamics and illuminate the distinct responses of fungal and bacterial necromass to biochar-induced changes in soil biogeochemical processes. However, the effects of biochar on MNC accumulation may vary between single-dose and repeated applications, influenced by changes in microbial community composition and activity. Therefore, long-term (>10 years) field experiments are essential to understand the mechanisms of microbially mediated SOC stabilization and optimize biochar application for sustainable soil management.

Acknowledgements

This work was financially supported by the National Natural Science Foundation of China (42277330 and 41877097), and the Science and Technology Innovation Special Fund of Jiangsu Province, China (BE2022304 and BE2022423).

Declaration of competing interest

The authors declare that they have no conflict of interest.

Declaration of generative AI and AI-assisted technologies in scientific writing

The authors declare that they did not use AI in the preparation and writing of this manuscript.

Appendices associated with this paper are available at https://doi.org/10.1016/j.jia.2025.10.001

References

Appuhn A, Joergensen R G. 2006. Microbial colonisation of roots as a function of plant species. *Soil Biology and Biochemistry*, **38**, 1040–1051.

Bach C E, Warnock D D, Van Horn D J, Weintraub M N, Sinsabaugh R L, Allison S D, German D P. 2013. Measuring phenol oxidase and peroxidase activities with pyrogallol, l-DOPA, and ABTS: Effect of assay conditions and soil type. *Soil Biology and Biochemistry*, **67**, 183–191.

Bao S D. 2000. *Soil and Agricultural Chemistry Analysis*. China Agriculture Press, Beijing. (in Chinese)

Barberán A, Bates S T, Casamayor E O, Fierer N. 2012. Using network analysis to explore co-occurrence patterns in soil microbial communities. *The ISME Journal*, **6**, 343–351.

Bossio D A, Scow K M. 1998. Impacts of carbon and flooding on soil microbial communities: Phospholipid fatty acid profiles and substrate utilization patterns. *Microbial Ecology*, **35**, 265–278.

Buckeridge K M, Creamer C, Whitaker J. 2022. Deconstructing the microbial necromass continuum to inform soil carbon sequestration. *Functional Ecology*, **36**, 1396–1410.

Buckeridge K M, La Rosa A F, Mason K E, Whitaker J, McNamara N P, Grant H K, Ostle N J. 2020a. Sticky dead microbes: Rapid abiotic retention of microbial necromass in soil. *Soil Biology and Biochemistry*, **149**, 107929.

Buckeridge K M, Mason K E, McNamara N P, Ostle N, Puissant J, Goodall T, Griffiths R I, Stott A W, Whitaker J. 2020b. Environmental and microbial controls on microbial necromass recycling, an important precursor for soil carbon stabilization. *Communications Earth & Environment*, **1**, 36.

Cai M K, Zhao G, Zhao B, Cong N, Zheng Z T, Zhu J T, Duan X Q, Zhang Y J. 2023. Climate warming alters the relative importance of plant root and microbial community in regulating the accumulation of soil microbial necromass carbon in a Tibetan alpine meadow. *Global Change Biology*, **29**, 3193–3204.

Cao D, Wang X X, Miao Y, Wu C F, Zhang H Q, Wang S, Wang F, Chen L, Liang C, Kuzyakov Y, Chen J P, Ge T D, Zhu Z K. 2025. Microbial strategies regulate organic carbon accumulation in saline paddy soils: A millennium chronosequence. *Catena*, **252**, 108869.

Chen R R, Senbayram M, Blagodatsky S, Myachina O, Dittert K, Lin X G, Blagodatskaya E, Kuzyakov Y. 2014. Soil C and N availability determine the priming effect: Microbial N mining and stoichiometric decomposition theories. *Global Change Biology*, **20**, 2356–2367.

Chen X B, Hu Y J, Xia Y H, Zheng S M, Ma C, Rui Y C, He H B, Huang D Y, Zhang Z H, Ge T D, Wu J S, Guggenberger G, Kuzyakov Y, Su Y R. 2021. Contrasting pathways of carbon sequestration in paddy and upland soils. *Global Change Biology*, **27**, 2478–2490.

Chen Y, Feng X Y, Zhao X, Hao X M, Tong L, Wang S F, Ding R S, Kang S Z. 2025. Biochar application enhances soil quality by improving soil physical structure under particular water and salt conditions in arid region of Northwest China. *Journal of Integrative Agriculture*, **24**, 3242–3263.

Chen Y L, Du Z L, Weng Z, Sun K, Zhang Y Q, Liu Q, Yang Y, Li Y, Wang Z B, Luo Y, Gao B, Chen B, Pan Z Z, Van Zwieten L. 2023a. Formation of soil organic carbon pool is regulated by the structure of dissolved organic matter and microbial carbon pump efficacy: A decadal study comparing different carbon management strategies. *Global Change Biology*, **29**, 5445–5459.

Chen Y L, Sun K, Yang Y, Gao B, Zheng H. 2023b. Effects of biochar on the accumulation of necromass-derived carbon, the physical protection and microbial mineralization of soil organic carbon. *Critical Reviews in Environmental Science and Technology*, **5**, 39–67.

Chen Z, Jin P H, Wang H, Hu T L, Lin X W, Xie Z B. 2022. Ecoenzymatic stoichiometry reveals stronger microbial carbon and nitrogen limitation in biochar amendment soils: A meta-analysis. *Science of the Total Environment*, **838**, 156532.

Cheng Z R, Guo J Y, Jin W, Liu Z T, Wang Q, Zha L, Zhou Z G, Meng Y L. 2024. Responses of SOC, labile SOC fractions, and amino sugars to different organic amendments in a coastal saline-alkali soil. *Soil and Tillage Research*, **239**, 106051.

Cui J, Zhu Z K, Xu X L, Liu S L, Jones D L, Kuzyakov Y, Shibistova O, Wu J S, Ge T D. 2020. Carbon and nitrogen recycling from microbial

necromass to cope with C:N stoichiometric imbalance by priming. *Soil Biology and Biochemistry*, **142**, 107720.
Daims H, Wagner M. 2018. Nitrospira. *Trends in Microbiology*, **26**, 462–463.
Dunbar J, Gallegos-Graves L V, Steven B, Mueller R, Hesse C, Zak D R, Kuske C R. 2014. Surface soil fungal and bacterial communities in aspen stands are resilient to eleven years of elevated CO_2 and O_3. *Soil Biology and Biochemistry*, **76**, 227–234.
Fan K K, Delgado-Baquerizo M, Guo X S, Wang D Z, Wu Y Y, Zhu M, Yu W, Yao H Y, Zhu Y G, Chu H Y. 2019. Suppressed N fixation and diazotrophs after four decades of fertilization. *Microbiome*, **7**, 143.
Feng X, Xia X, Chen S T, Lin Q M, Zhang X H, Cheng K, Liu X Y, Bian R J, Zheng J F, Li L Q, Joseph S, Drosos M, Pan G X. 2022. Amendment of crop residue in different forms shifted micro-pore system structure and potential functionality of macroaggregates while changed their mass proportion and carbon storage of paddy topsoil. *Geoderma*, **409**, 115643.
Fierer N, Bradford M A, Jackson R B. 2007. Toward an ecological classification of soil bacteria. *Ecology*, **88**, 1354–1364.
Gai X P, Wang H Y, Liu J, Zhai L M, Liu S, Ren T Z, Liu H B. 2014. Effects of feedstock and pyrolysis temperature on biochar adsorption of ammonium and nitrate. *PLoS ONE*, **9**, e113888.
Gao S, DeLuca T H, Cleveland C C. 2019. Biochar additions alter phosphorus and nitrogen availability in agricultural ecosystems: A meta-analysis. *Science of the Total Environment*, **654**, 463–472.
German D P, Weintraub M N, Grandy A S, Lauber C L, Rinkes Z L, Allison S D. 2011. Optimization of hydrolytic and oxidative enzyme methods for ecosystem studies. *Soil Biology and Biochemistry*, **43**, 1387–1397.
Gong Z T. 1999. *Chinese Soil Taxonomy*: *Theory Approaches and Application*. Science Press, Beijing, China. pp. 160–165. (in Chinese)
Han Z Q, Xu P S, Li Z T, Guo S M, Li S Q, Liu S W, Wu S, Wang J Y, Zou J W. 2023. Divergent effects of biochar amendment and replacing mineral fertilizer with manure on soil respiration in a subtropical tea plantation. *Biochar*, **5**, 73.
He M, Fang K, Chen L Y, Feng X H, Qin S Q, Kou D, He H B, Liang C, Yang Y H. 2022. Depth-dependent drivers of soil microbial necromass carbon across Tibetan alpine grasslands. *Global Change Biology*, **28**, 936–949.
Heuck C, Weig A, Spohn M. 2015. Soil microbial biomass C:N:P stoichiometry and microbial use of organic phosphorus. *Soil Biology and Biochemistry*, **85**, 119–129.
Hill P W, Jones D L. 2019. Plant–microbe competition: Does injection of isotopes of C and N into the rhizosphere effectively characterise plant use of soil N? *New Phytologist*, **221**, 796–806.
Hu P L, Zhang W, Kuzyakov Y, Xiao L M, Xiao D, Xu L, Chen H S, Zhao J, Wang K L. 2023. Linking bacterial life strategies with soil organic matter accrual by karst vegetation restoration. *Soil Biology and Biochemistry*, **177**, 108925.
Hu Y, Zheng Q, Zhang S S, Noll L, Wanek W. 2018. Significant release and microbial utilization of amino sugars and D-amino acid enantiomers from microbial cell wall decomposition in soils. *Soil Biology and Biochemistry*, **123**, 115–125.
Hu Y T, Zheng Q, Noll L, Zhang S S, Wanek W. 2020. Direct measurement of the in situ decomposition of microbial-derived soil organic matter. *Soil Biology and Biochemistry*, **141**, 107660.
Huang W G, Kuzyakov Y, Niu S L, Luo Y, Sun B, Zhang J B, Liang Y T. 2023. Drivers of microbially and plant-derived carbon in topsoil and subsoil. *Global Change Biology*, **29**, 6188–6200.
Jia X Y, Ma H Z, Yan W M, Shangguan Z, Zhong Y. 2024. Effects of co-application of biochar and nitrogen fertilizer on soil profile carbon and nitrogen stocks and their fractions in wheat field. *Journal of Environmental Management*, **368**, 122140.
Jiang B N, Lu M B, Zhang Z Y, Xie B L, Song H L. 2023. Quantifying biochar-induced greenhouse gases emission reduction effects in constructed wetlands and its heterogeneity: A multi-level meta-analysis. *Science of the Total Environment*, **855**, 158688.
Joergensen R G. 2018. Amino sugars as specific indices for fungal and bacterial residues in soil. *Biology and Fertility of Soils*, **54**, 559–568.
Ju F, Xia Y, Guo F, Wang Z P, Zhang T. 2014. Taxonomic relatedness shapes bacterial assembly in activated sludge of globally distributed wastewater treatment plants. *Environmental Microbiology*, **16**, 2421–2432.
Kerner P, Struhs E, Mirkouei A, Aho K, Lohse K, Dungan R, You Y Q. 2023. Microbial responses to biochar soil amendment and influential factors: A three-level meta-analysis. *Environmental Science & Technology*, **57**, 19838–19848.
Koele N, Bird M, Haig J, Marimon-Junior B H, Marimon B S, Phillips O L, de Oliveira E A, Quesada C A, Feldpausch T R. 2017. Amazon Basin forest pyrogenic carbon stocks: First estimate of deep storage. *Geoderma*, **306**, 237–243.
Kong F X, Jiu A M, Kan Z R, Zhou J, Yang H S, Li F M. 2024. Deep tillage combined with straw biochar return increases rice yield by improving nitrogen availability and root distribution in the subsoil. *Field Crops Research*, **315**, 109481.
Lehmann J, Cowie A, Masiello C A, Kammann C, Woolf D, Amonette J E, Cayuela M L, Camps-Arbestain M, Whitman T. 2021. Biochar in climate change mitigation. *Nature Geoscience*, **14**, 883–892.
Lehmann J, Rillig M C, Thies J, Masiello C A, Hockaday W C, Crowley D. 2011. Biochar effects on soil biota – A review. *Soil Biology and Biochemistry*, **43**, 1812–1836.
Lei C T, Lu T, Qian H F, Liu Y X. 2023. Machine learning models reveal how biochar amendment affects soil microbial communities. *Biochar*, **5**, 89.
Li H, Yang S, Semenov M V, Yao F, Ye J, Bu R C, Ma R A, Lin J J, Kurganova I, Wang X G, Deng Y, Kravchenko I, Jiang Y, Kuzyakov Y. 2021. Temperature sensitivity of SOM decomposition is linked with a K-selected microbial community. *Global Change Biology*, **27**, 2763–2779.
Li M R, Zhang X F, Xin X L, Yang W L, Zhong X Y, Liu Y C, Zhu A N. 2024. Characteristics of organic amendments induce diverse microbial metabolisms for exogenous C turnover in Mollisols. *Applied Soil Ecology*, **203**, 105681.
Li P H, Hur J. 2017. Utilization of UV-Vis spectroscopy and related data analyses for dissolved organic matter (DOM) studies: A review. *Critical Reviews in Environmental Science and Technology*, **47**, 131–154.
Li T T, Yuan Y, Mou Z J, Li Y, Kuang L H, Zhang J, Wu W J, Wang F M, Wang J, Lambers H, Sardans J, Peñuelas J, Ren H, Liu Z F. 2023. Faster accumulation and greater contribution of glomalin to the soil organic carbon pool than amino sugars do under tropical coastal forest restoration. *Global Change Biology*, **29**, 533–546.
Li Z, Duan X, Guo X B, Gao W, Li Y, Zhou P, Zhu Q H, O'Donnell A G, Dai K, Wu J S. 2024. Microbial metabolic capacity regulates the accrual of mineral-associated organic carbon in subtropical paddy soils. *Soil Biology and Biochemistry*, **195**, 109457.
Liang C, Amelung W, Lehmann J, Kästner M. 2019. Quantitative assessment of microbial necromass contribution to soil organic matter. *Global Change Biology*, **25**, 3578–3590.
Liang C, Schimel J P, Jastrow J D. 2017. The importance of anabolism in microbial control over soil carbon storage. *Nature Microbiology*, **2**, 17105.
Liu H Y, Mi Z R, Lin L, Wang Y H, Zhang Z H, Zhang F W, Wang H, Liu L L, Zhu B, Cao G M, Zhao X Q, Sanders N J, Classen A T, Reich P B, He J S. 2018. Shifting plant species composition in response to climate change stabilizes grassland primary production. *Proceedings of the National Academy of Sciences of the United States of America*, **115**, 4051–4056.
Liu Y L, Ge T D, van Groenigen K J, Yang Y H, Wang P, Cheng K, Zhu Z K, Wang J K, Li Y, Guggenberger G, Sardans J, Penuelas J, Wu J S, Kuzyakov Y. 2021. Rice paddy soils are a quantitatively important carbon store according to a global synthesis. *Communications Earth & Environment*, **2**, 154.
Liu Y L, Ge T D, Zhu Z K, Liu S L, Luo Y, Li Y, Wang P, Gavrichkova O, Xu X L, Wang J K, Wu J S, Guggenberger G, Kuzyakov Y. 2019. Carbon input and allocation by rice into paddy soils: A review. *Soil Biology and Biochemistry*, **133**, 97–107.
Liu Z W, Wu X L, Li S X, Liu W, Bian R J, Zhang X H, Zheng J F, Drosos M, Li L Q, Pan G X. 2021. Quantitative assessment of the effects of biochar amendment on photosynthetic carbon assimilation and dynamics in a rice–soil system. *New Phytologist*, **232**, 1250–1258.
Liu Z W, Wu X L, Liu W, Bian R J, Ge T D, Zhang W, Zheng J F, Drosos M, Liu X Y, Zhang X H, Cheng K, Li L Q, Pan G X. 2020. Greater microbial carbon use efficiency and carbon sequestration in soils: Amendment of biochar versus crop straws. *GCB Bioenergy*, **12**, 1092–1103.
Liu Z W, Zhu M T, Wang J M, Liu X X, Guo W J, Zheng J F, Bian R J,

Wang G M, Zhang X H, Cheng K, Liu X Y, Li L Q, Pan G X. 2019. The responses of soil organic carbon mineralization and microbial communities to fresh and aged biochar soil amendments. *GCB Bioenergy*, **11**, 1408–1420.

Ma R L, Wu X L, Liu Z W, Yi Q, Xu M, Zheng J F, Bian R J, Zhang X H, Pan G X. 2023. Biochar improves soil organic carbon stability by shaping the microbial community structures at different soil depths four years after an incorporation in a farmland soil. *Current Research in Environmental Sustainability*, **5**, 100214.

Ma Y Q, Woolf D, Fan M S, Qiao L, Li R, Lehmann J. 2023. Global crop production increase by soil organic carbon. *Nature Geoscience*, **16**, 1159–1165.

Major J, Lehmann J, Rondon M, Goodale C. 2010. Fate of soil-applied black carbon: Downward migration, leaching and soil respiration. *Global Change Biology*, **16**, 1366–1379.

Malik A A, Martiny J B H, Brodie E L, Martiny A C, Treseder K K, Allison S D. 2020. Defining trait-based microbial strategies with consequences for soil carbon cycling under climate change. *The ISME Journal*, **14**, 1–9.

Nan Q, Tang L P, Chi W C, Waqas M, Wu W X. 2023. The implication from six years of field experiment: The aging process induced lower rice production even with a high amount of biochar application. *Biochar*, **5**, 27.

Novak J, Busscher W, Watts D W, Amonette J, Ippolito J, Lima I, Gaskin J, Das K C, Steiner C, Ahmedna M, Rehrah D, Schomberg H. 2012. Biochars impact on soil-moisture storage in an Ultisol and two Aridisols. *Soil Science*, **177**, 310–320.

Parks D H, Tyson G W, Hugenholtz P, Beiko R G. 2014. STAMP: Statistical analysis of taxonomic and functional profiles. *Bioinformatics*, **30**, 3123–3124.

Qin S Q, Chen L Y, Fang K, Zhang Q W, Wang J, Liu F T, Yu J C, Yang Y H. 2019. Temperature sensitivity of SOM decomposition governed by aggregate protection and microbial communities. *Science Advances*, **5**, eaau1218.

R Core Team. 2022. *R*: *A Language and Environment for Statistical Computing*. R Foundation for Statistical Computing, Vienna, Austria.

Schweigert M, Herrmann S, Miltner A, Fester T, Kästner M. 2015. Fate of ectomycorrhizal fungal biomass in a soil bioreactor system and its contribution to soil organic matter formation. *Soil Biology and Biochemistry*, **88**, 120–127.

Shao P S, Lynch L, Xie H T, Bao X L, Liang C. 2021. Tradeoffs among microbial life history strategies influence the fate of microbial residues in subtropical forest soils. *Soil Biology and Biochemistry*, **153**, 108112.

Shi W, Ju Y Y, Bian R J, Li L Q, Joseph S, Mitchell D R G, Munroe P, Taherymoosavi S, Pan G X. 2020. Biochar bound urea boosts plant growth and reduces nitrogen leaching. *Science of the Total Environment*, **701**, 134424.

Sinsabaugh R L, Lauber C L, Weintraub M N, Ahmed B, Allison S D, Crenshaw C, Contosta A R, Cusack D, Frey S, Gallo M E, Gartner T B, Hobbie S E, Holland K, Keeler B L, Powers J S, Stursova M, Takacs-Vesbach C, Waldrop M P, Wallenstein M D, Zak D R, *et al.* 2008. Stoichiometry of soil enzyme activity at global scale. *Ecology Letters*, **11**, 1252–1264.

Sinsabaugh R L, Manzoni S, Moorhead D L, Richter A. 2013. Carbon use efficiency of microbial communities: Stoichiometry, methodology and modelling. *Ecology Letters*, **16**, 930–939.

Sohi S P. 2012. Carbon storage with benefits. *Science*, **338**, 1034–1035.

Takele L, Yang S Y, Chen Z M, Yuan J J, Ding W X. 2025. Contribution of microbial necromass to soil organic carbon in profile depths exhibited opposite patterns across ecosystems: A global meta-analysis. *Soil Biology and Biochemistry*, **207**, 109842.

Wang B R, An S S, Liang C, Liu Y, Kuzyakov Y. 2021. Microbial necromass as the source of soil organic carbon in global ecosystems. *Soil Biology and Biochemistry*, **162**, 108422.

Wang C, Qu L R, Yang L M, Liu D W, Morrissey E, Miao R H, Liu Z P, Wang Q K, Fang Y T, Bai E. 2021. Large-scale importance of microbial carbon use efficiency and necromass to soil organic carbon. *Global Change Biology*, **27**, 2039–2048.

Wang J Y, Xiong Z Q, Kuzyakov Y. 2016. Biochar stability in soil: Meta-analysis of decomposition and priming effects. *GCB Bioenergy*, **8**, 512–523.

Wang J X, Huang Q, Peng K, Yang D Y, Wei G Z, Ren Y F, Wang Y X, Wang X K, Vinay N, Sun S K, Yang Y M, Mo F. 2024. Biochar induced trade-offs and synergies between ecosystem services and crop productivity. *Journal of Integrative Agriculture*, **23**, 3882–3895.

Wang R, Hou J H, Chen L T, He L L, Na L P, Wang Y Y, Lu H H, Yang S M, Liu Y X. 2025. Priming effects of vermiculite modified rice straw biochar on soil organic carbon: A new perspective of soil bacteria. *Biochar*, **7**, 54.

Wang X X, Zhou L Y, Zhou G Y, Zhou H M, Lu C Y, Gu Z Z, Liu R Q, He Y H, Du Z G, Liang X N, He H B, Zhou X H. 2022. Tradeoffs of fungal and bacterial residues mediate soil carbon dynamics under persistent drought in subtropical evergreen forests. *Applied Soil Ecology*, **178**, 104588.

Wang Y, Yin Y J, Joseph S, Flury M, Wang X, Tahery S, Li B G, Shang J Y. 2024. Stabilization of organic carbon in top- and subsoil by biochar application into calcareous farmland. *Science of the Total Environment*, **907**, 168046.

Weng Z H, Lehmann J, Zwieten L van, Joseph S, Archanjo B S, Cowie B, Thomsen L, Tobin M J, Vongsvivut J P, Klein A, Doolette C L, Hou H, Mueller C W, Lombi E, Kopittke P M. 2021. Probing the nature of soil organic matter. *Critical Reviews in Environmental Science and Technology*, **52**, 4072–4093.

Xia L L, Cao L, Yang Y Y, Ti C P, Liu Y Z, Smith P, van Groenigen K J, Lehmann J, Lal R, Butterbach-Bahl K, Kiese R, Zhuang M, Lu X, Yan X. 2023. Integrated biochar solutions can achieve carbon-neutral staple crop production. *Nature Food*, **4**, 236–246.

Yang L Y, Canarini A, Zhang W S, Lang M, Chen Y X, Cui Z L, Kuzyakov Y, Richter A, Chen X P, Zhang F S, Tian J. 2024. Microbial life-history strategies mediate microbial carbon pump efficacy in response to N management depending on stoichiometry of microbial demand. *Global Change Biology*, **30**, e17311.

Yang Y, Gunina A, Cheng H, Liu L X, Wang B R, Dou Y X, Wang Y Q, Liang C, An S S, Chang SX. 2025. Unlocking mechanisms for soil organic matter accumulation: Carbon use efficiency and microbial necromass as the keys. *Global Change Biology*, **31**, e70033.

Yao Q, Liu J J, Yu Z H, Li Y S, Jin J, Liu X B, Wang G H. 2017. Three years of biochar amendment alters soil physiochemical properties and fungal community composition in a black soil of northeast China. *Soil Biology and Biochemistry*, **110**, 56–67.

Yuan Y H, Liang Y, Cai H G, Yuan J C, Li C L, Liu H, Zhang C, Wang L C, Zhang J J. 2025. Soil organic carbon accumulation mechanisms in soil amended with straw and biochar: Entombing effect or biochemical protection? *Biochar*, **7**, 33.

Zhang X D, Amelung W. 1996. Gas chromatographic determination of muramic acid, glucosamine, mannosamine, and galactosamine in soils. *Soil Biology and Biochemistry*, **28**, 1201–1206.

Zhang Y Y, Wang T, Yan C, Li Y Z, Mo F, Han J. 2024. Microbial life-history strategies and particulate organic carbon mediate formation of microbial necromass carbon and stabilization in response to biochar addition. *Science of the Total Environment*, **950**, 175041.

Zhu C H, Xiang J, Zhang Y P, Zhang Y K, Zhu D D, Chen H Z. 2019. Mechanized transplanting with side deep fertilization increases yield and nitrogen use efficiency of rice in Eastern China. *Scientific Reports*, **9**, 5653.

Zhu M T, Liu Z W, Yi Q, Ma R L, Xu M, Song K Y, Bian R J, Zheng J F, Zhang X H. 2025. The divergent response of fungal and bacterial necromass carbon in soil aggregates under biochar amendment in paddy soil. *Plant and Soil*, **531**, 993–1008.

Executive Editor-in-Chief Keke Yi
Managing Editor Lujuan Sun